DRY THERMAL CONVECTION – DATA ANALYSIS AND INTERPRETATION

by A. G. Williams

Flinders Institute of Atmospheric and Marine Services, South Australia

Presented at the XX OSTIV Congress, Benalla, Australia (1987)

Summary

Two models are presented, simulating the statistics of a field of thermals rising into a Convective Boundary Layer. The second is a three-dimensional model, designed to reconstruct the temperature, vertical velocity, and area-related statistics of an airplane flight-path through the field.

Measurements are taken of the convective regime over a semi-arid region in South Australia, under conditions of dry, shallow convection. Problems of analysis of flight-collected data are discussed, and the results from the field experiment are compared with the models.

1. Introduction

When flow in the Planetary Boundary Layer is dominated by convective turbulence, the layer is often referred to as the Convective Boundary Layer (CBL). Over land, this convection is often driven primarily by the surface heat flux, rather than the moisture flux. Under these conditions (Bowen Ratio > 1), moisture acts as a passive scalar, and we have "Dry Convection."

Transfer of heat, moisture and momentum between the surface and the overlying CBL is accomplished to a large extent by discrete convective elements called "thermals," which form over surfaces which are considerably warmer than the overlying air. The nature of thermals is an often discussed subject, and it is clear that they take many different shapes and forms in reality. This paper presents some of the findings of a study by the author into the techniques of analysis and interpretation of flight-collected data as applied to the subject of dry thermal convection in the CBL over land.

Measurements were taken using an instrumented aircraft, and the results were compared with two mathematical models via a series of statistical parameters and specialized analytical techniques.

To facilitate easy comparison with results of other studies, the findings are presented as normalized profiles, using scaling parameters dictated by Mixed-Layer Similarity theory. The Mixed Layer is the layer in the CBL, above the Surface and Free Convection Layers, where the structure of the turbulence is governed only by the physical parameters H (boundary layer depth), Q_0 (surface heat flux), and $g/\bar{\theta}$ (buoyancy parameter). Our study was mainly concerned with this layer, where the scaling velocities are w_* and T_*, given by:

$$w_* = \left[H \frac{g}{\bar{\theta}} \overline{\theta' w_0'} \right]^{\frac{1}{3}}, \quad Q_0 = \rho C_p \overline{\theta' w_0'}$$

$$T_* = \frac{\overline{\theta' w_0'}}{w_*}$$

The main aims of the study were to explore new ways in which airborne sensor data can be realistically interpreted and compared with ideality, and to identify and suggest solutions to some of the problems involved.

2. The Models

2.1 Vertical Structure

Two mathematical models are used in this study. The first is a one dimensional model derived by Manton (1978), which describes the way in which the physical quantities associated with a (dry) thermal change as it ascends through the Mixed

Layer. He derives equations for mass and momentum balance involving the effects of buoyancy and entrainment of environmental air. Manton showed that, although the model is somewhat simplified, the predicted profiles it produces compare quite favourably with actual Mixed Layer data. A major advantage of this model is that it provides analytical solutions to the governing equations.

The major assumptions of the model are as follows. The thermals interact with their environment in order to maintain a constant area fraction. This has been the observation of many groups, and Manton (1977) suggests a representative value for this fraction, of $\Delta_0 = 0.42$. The behavior of a thermal is determined primarily by local conditions, and so the total derivatives (d/dt) may be approximated by local advection terms ($w\ \partial/\partial z$). Also, it is assumed that volume is conserved (so that the vertical velocity averaged over the thermal and its environment, is zero). Lastly, the analysis ignores all effects of background turbulence, and implicitly assumes "top-hat" profiles for all the variables.

The analytical solutions to his model equations, are as follows. If we define the intermediate function,

$$F(z/H) = \left[\alpha_3^3 + \frac{3}{4}[1 - (1 - z/H)^2)]\right]^{\frac{1}{3}}$$

then:

$$\frac{w_i}{w_*} = F(z/H)\ ,\quad \frac{\theta_1}{\theta_*} = (1 - z/H)\,F(z/H)^{-1}\ ,\quad \frac{a}{a_0} = F(z/H)^{1-\Delta_0}$$

where w_i is vertical velocity inside thermals, θ_1 is the deviation from the overall mean of potential temperature inside thermals, a is cross-sectional area, a_0 is the cross-sectional area at $w_i = w_*$, and $\alpha_3 = w_i/w_*$ at $z=0$.

From these solutions, we see that thermals accelerate throughout the Mixed Layer. The temperature excess decreases with height due to entrainment, and the profile of cross-sectional area is consistent with the observations of Warner and Telford (1967), in that the size of thermals varies very little with height in the bulk of the Mixed Layer, with gross changes in size only occurring very close to the surface.

2.2 Horizontal Structure

By its very nature, the data obtained from an airborne sensor system is not two-dimensional, but one-dimensional. The record produced will represent a one-dimensional cut through the turbulent field. Because of this, it is often asked, "how representative of the overall picture are our data?" Over a long flight-path, many statistical quantities may "even out" to give truly representative results. However, some quantities may not. For example, because the flight path will seldom cut directly through the centre of a thermal, the average length of thermal sections in the record will always be less than the average diameter of the thermals flown through. In view of such questions, a second model was constructed to simulate a (horizontal) flight path through a three-dimensional field of thermals.

Since the vertical variations of thermal quantities seem quite well described by the first model (to the extent of our needs), we introduced them into the second model, and applied new functions to them describing the variations in the horizontal. This was done in the following way.

Three-dimensional Gaussian curves were used as "smoothing functions," to translate the strength of the thermals, as predicted by the first model, onto the horizontal plane. The Gaussian profiles need to be steep, though, to maintain the thermals as well-defined phenomena with steep gradients at the edges. The three-dimensional velocity profile used, was:

$w = w_0 + w_e + G(r,\sigma)(w_i - w_e)$

where G is the Gaussian distribution function,

$$G(r,\sigma) = c\ e^{-\frac{1}{2}\left[\frac{r}{\sigma}\right]^2}$$

and r is the radius from the centre, c=1 for normalisation, σ is the standard deviation (a measure of the "fatness" of the distribution), w_e is the vertical velocity outside the thermal as predicted by the first model, and w_0 is a moderating velocity which ensures that the net vertical velocity over the plane is zero.

It can be shown that the above equation for velocity reduces to:

$$\frac{w}{w_*} = \frac{w_0}{w_*} + (G(r,\sigma)(1 + \alpha_1) - \alpha_1)\,F(z/H)$$

where $\alpha_1 \sim 0.72$. Similarly, the potential temperature is given by:

$$\frac{\theta'}{\theta_*} = \frac{\theta_0}{\theta_*} + (G(r,\sigma)(1 + \alpha_1) - \alpha_1)(1 - z/H)\,F^{-1}(z/H)$$

and the change of size with height is given by:

$\sigma(z/H) = \sigma_{max} A(z/H)$

where $A(z/H) = a/a_0 = F(z/H)^{1-\Delta_0}$.

The model was constructed in such a way that a user could introduce a field of thermals at given locations on the surface of the grid, with differing sizes, and propagate them upwards into the boundary layer, measuring a number of statistical quantities for the whole field by sampling along the grid lines. Tuning of the model was required for any one set of thermals introduced by the user. This was done by adjusting the standard deviations (σ) of the thermals, until the total fractional area occupied by thermals at $z/H=0.5$, became equal to the $\Delta_0 = 0.42$ suggested by Manton.

The model was run using a random field of 50 thermals, each with a maximum deviation of $\sigma_{max} = 0.05$ (chosen by tuning requirements). These were propagated vertically through 50 heights to the top of the boundary layer. The grid contained 50*50 data points, and thermals were defined by a threshold of 0.5 standard deviations above the mean.

Figures 1 and 2 are contour plots and hidden-line views of the vertical velocity field at the height $z/H=0.5$. The results from this model run will be used in section 4 to compare with some real data.

3. Data, Techniques and Definitions

On Monday, May 26, 1986, data were collected in a series of runs over the Hinck's Conservation Park, on Eyre Peninsula, South Australia, under conditions of dry, shallow convection. The aircraft used was the research aircraft owned by F.I.A.M.S. (Flinders Institute of Atmospheric and Marine Science), the Grob G109B motorglider, under the command of Dr. Jorg Hacker, and assisted by the author. Each flight leg was approximately 40 km long, and there were six flight levels, from near the surface to $z/H \sim 0.7$. The average flight speed was around 80 knots, and the data were sampled at 13 Hz, corresponding to a rough sampling distance of 2.3 metres per sample for north-bound legs, and 3.8 metres per sample for south-bound legs.

There was a strong potential temperature inversion present, the base of which was at about H-840 metres. Associated with

FIGURE 1. Contour Plot of Vertical Velocity at z/H=0.5 for 50-thermal study. Dotted lines are <0.0. "North-East" view. Contour interval $w/w_* = 0.2$.

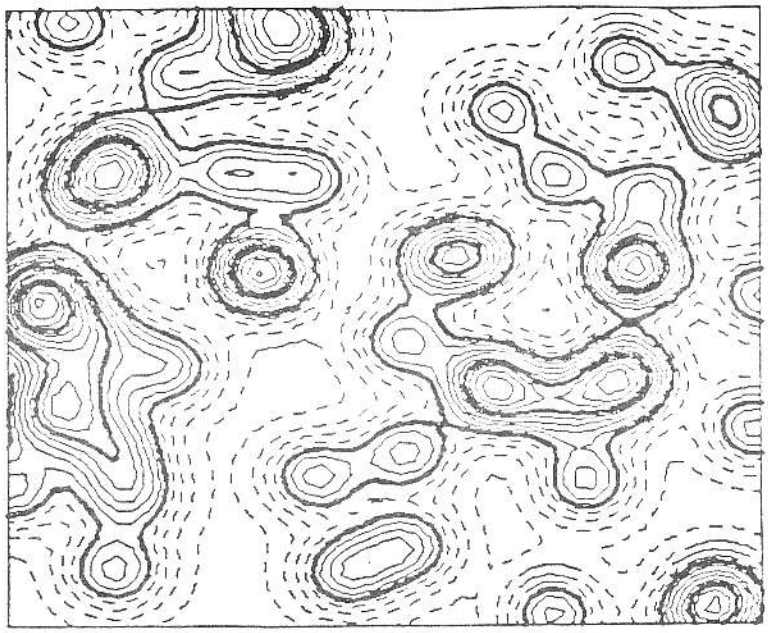

FIGURE 2. Hidden-line view of the above field.

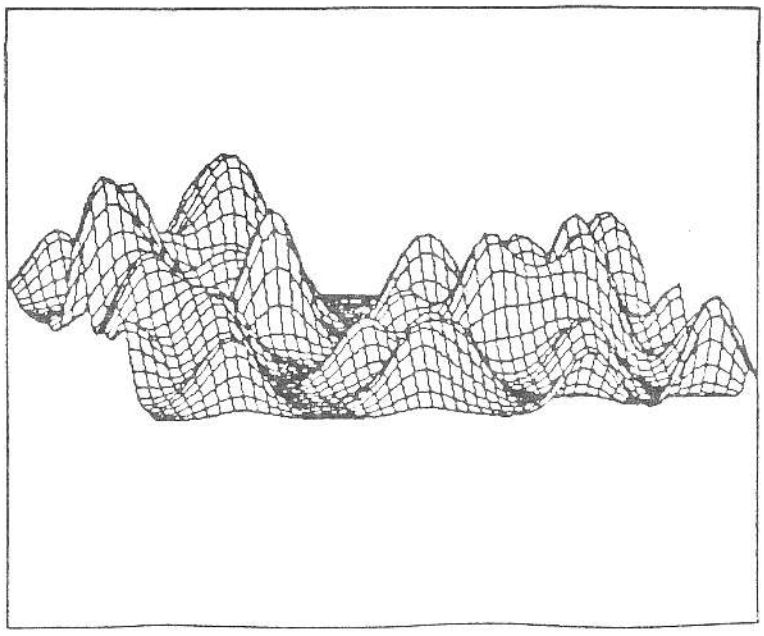

the inversion was a major drop in turbulence, and a sharp decrease in humidity. Below this inversion, the atmosphere supported almost constant profiles of potential temperature and specific humidity. The flux profiles were calculated from the data, and the surface fluxes were estimated to be 60 w/m² for the sensible heat, and 30 w/m² for the latent heat, giving a surface Bowen ratio of about 2.

To eliminate the effects of linear and meso-scale variations, the time series were high-pass filtered with a symmetrical Lanczos square-taper filter with 1001 weights and a cutoff frequency corresponding to a wavelength of 5 km. To eliminate the effects of high frequency noise interfering with the assessment of thermal events by the programs, the time series were also low-pass filtered with a similar filter, and a cutoff frequency corresponding to about 80m. The author notes that in more rigorous studies, especially close to the surface, the use of low-pass filters should be set under scrutiny, as their effect on the time series can often be quite dependant on small changes in the cutoff frequency. For the purposes of this study, however, low-pass filtering was found to be sufficient, and figure 3 gives an example of its effects.

Potential temperature was used as the tracer of thermals, in preference to humidity (which acts as a passive scalar in dry convection) and vertical velocity (the fluctuations of which, both within and outside thermals, may be larger than the mean thermal updraft velocity). Thermal events were identified in the record, by requiring that θ be greater than or equal to a threshold value, given by half a standard deviation above the mean.

4. Results and Comparisons

We now present some of the results obtained from the comparison of the model results with the field data.

Figure 4 presents the overall standard deviation of potential temperature as measured in the field, and compared with the predictions of the two models. The field data compare quite well. We note that the models predict very similar profiles, which is pleasing, since the aim in constructing the second model was not so much to improve on the predictions of the first model, but rather to provide predictions that the first model could not.

Figure 5 compares the predicted average potential temperature inside thermals with the real data. Again, the comparison is quite good, and the models predict almost identical profiles.

We now come to the statistics that could be predicted from the second model but not the first. The ratio of the standard deviation of temperatures inside thermals to the overall standard deviation (thermal and environment) is given in Figure 6. The model predicts an almost constant ratio with height. The actual data are very scattered, but clearly fall mainly to the left of the curve, showing that the amount of variance of temperature inside thermals is actually less than predicted! This indicates that the typical "shape" of thermals probably lies between the top-hat shape of the first model and the Gaussian shape of the second. More complex shapes for thermals could easily be incorporated into the second model, simply by

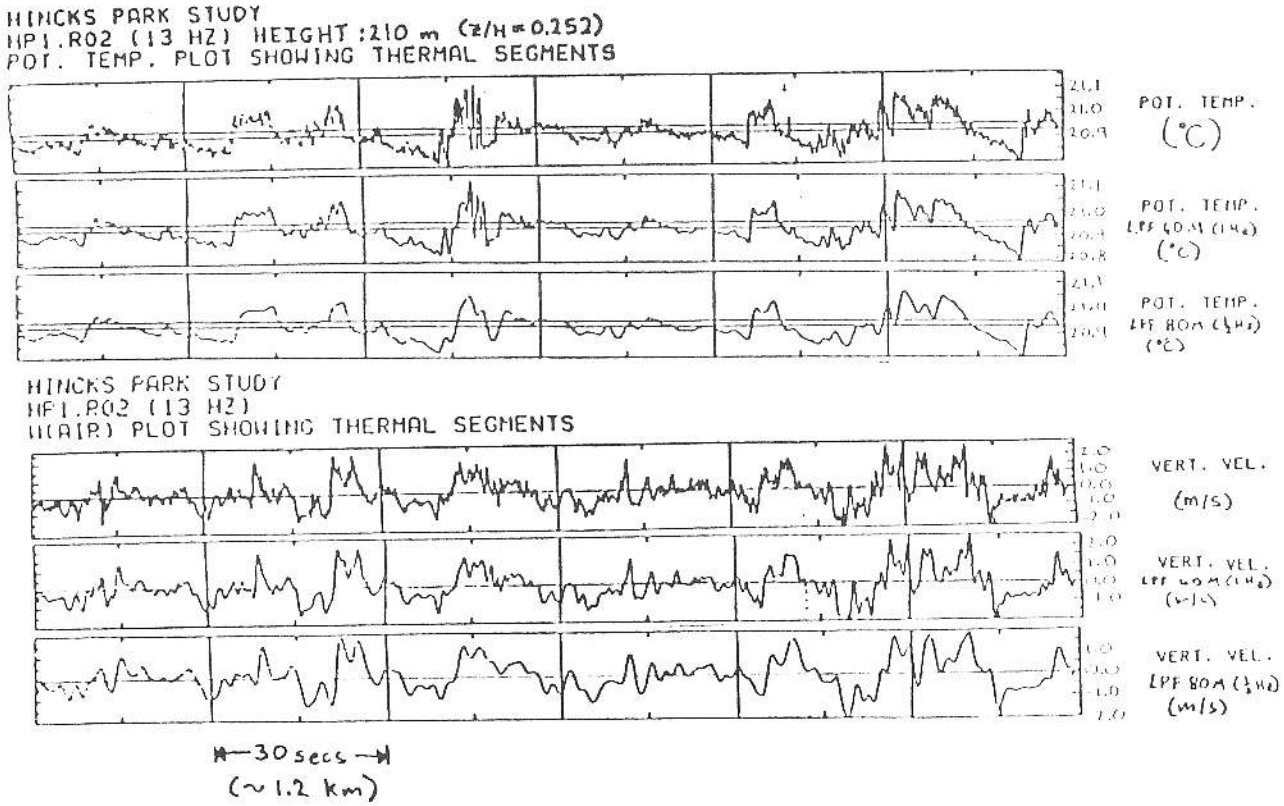

FIGURE 3. The effects of filtering the θ and w time series, with cutoff wavelengths of 40 and 80 m.

FIGURE 4. Standard deviation of potential temperature compared with the models.

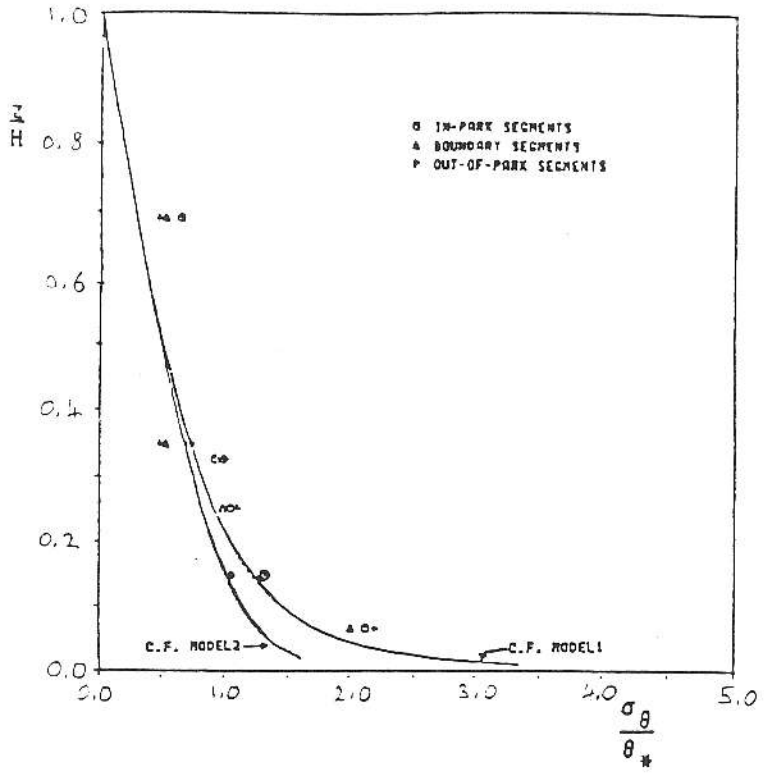

FIGURE 5. Average potential temperature for segments above threshold.

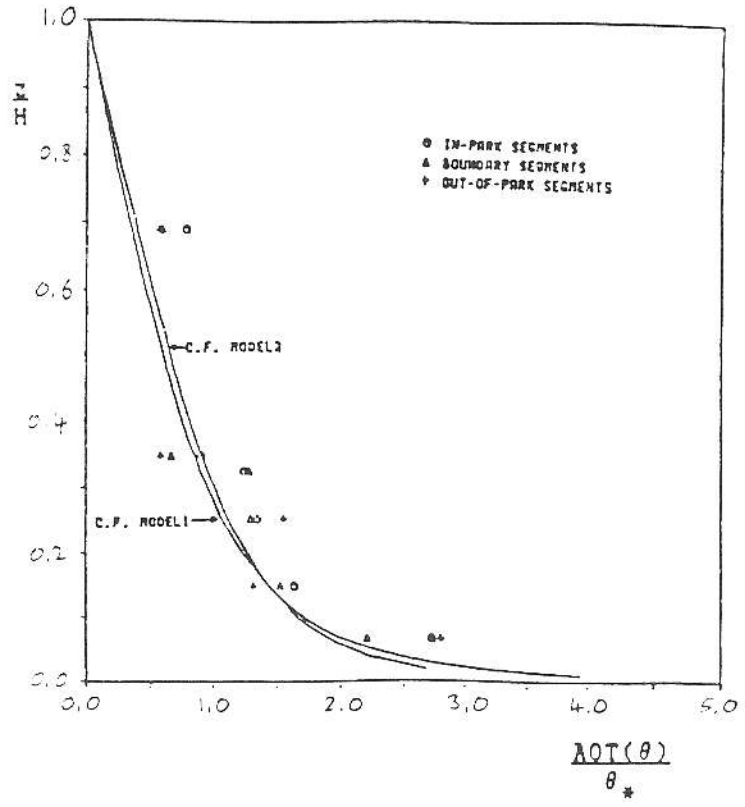

FIGURE 6. Ratio of the standard deviation of temperature inside thermals to the overall temperature standard deviation.

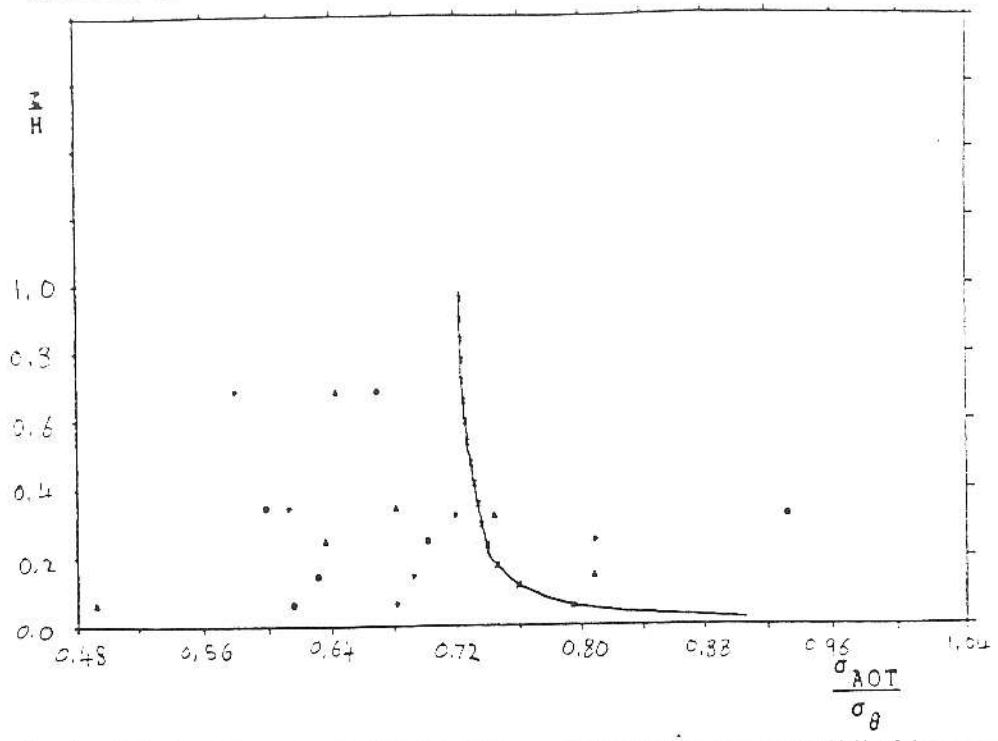

adjusting the function $G(r,\sigma)$. A thermal with sharper sides and a flatter top could be used, for example, or even a "double-peaked" thermal.

Figure 7 presents the ratio of the standard deviation of linear-area of thermals (length of thermal segments in the record) to the average. The contribution of the model represents the effect of flying through random chords of thermals rather than only centres. It predicts an almost constant ratio with height: the standard deviation is 50-60% of the average segment length. All of the real data points lie to the right of this curve, as expected, and the differences between the data points and the model curve represent the contributions to the standard deviation due to other effects (such as real differences in thermal diameter, and background turbulence). The data are again very scattered, and no further conclusions can really be made on this point from the present data set.

FIGURE 7. Ratio of the standard deviation of linear-area of thermal segments to the average.

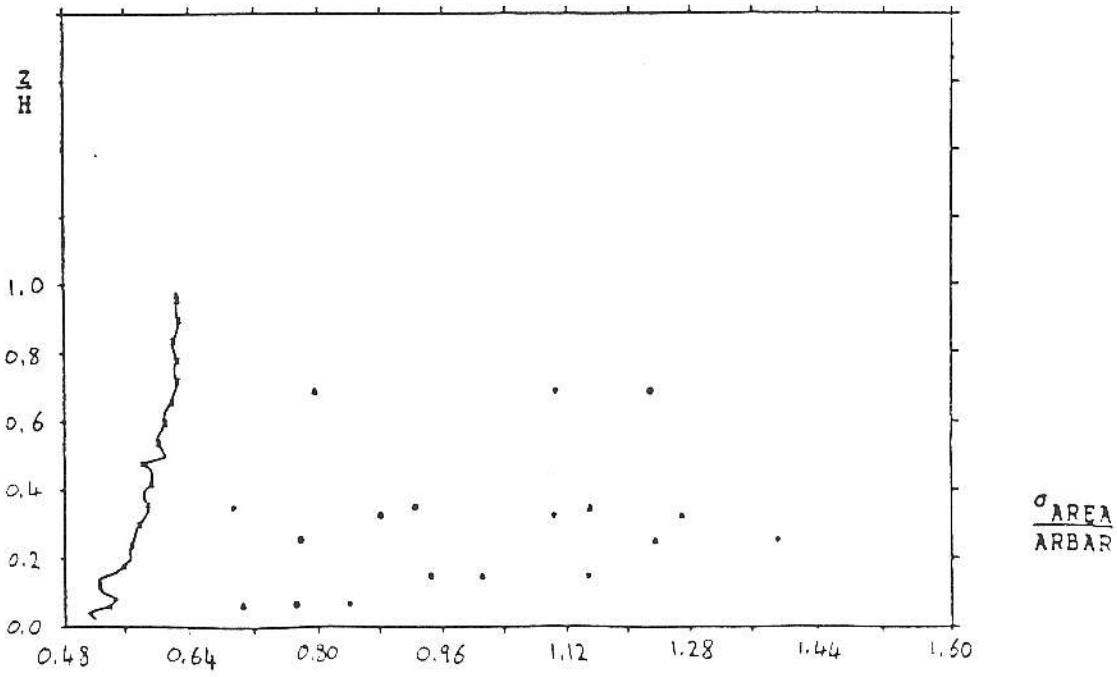

Figures 8 and 9 depict the profiles of mean segment length as predicted by the model (Figure 8) and as measured in the field (Figure 9). They do not appear on the same graph because they can be compared only in shape, and not in magnitude (due to the arbitrary nature of the model). Both figures clearly show the expansion of thermals as they rise into the CBL and entrain environmental air. The "bumpiness" of the model curve is due to edge effects on the grid. This could probably be removed by running the model using several different random distributions, and taking their average. The real data plot (Figure 9) was computed from the humidity record, rather than the θ record. This is because it was found that the length ("area") related statistics were best computed from the humidity record. Towards the top of the CBL, temperature becomes a less-reliable tracer of thermals, since warmer air from the penetration layer may mix with the environment, causing the temperature excess to be reduced. This problem does not occur in the humidity trace, since the air from above is drier, and so would actually accentuate the differences between thermals and their environments. Although humidity cannot strictly be used as the tracer in dry convection, its action as a "passive scalar" means that it can be used to look at length-related statistics. This seems to be the reason why it was found to be useful in this aspect (little scatter), whereas it displayed enormous scatter in all the other statistics.

5. Conclusions

This work was not intended to offer any new contribution to the physics of the subject. Rather, it has been directed at exploring the prospect of using a simple three-dimensional analytical model in the realistic interpretation of airborne sensor data by comparison with (controlled) ideality. The design of the (second) model is such that many doors are left open for future use. Studies of the effects of introducing many kinds of

FIGURE 8. Average Linear-Area of thermal segments over velocity threshold (50-thermal study)

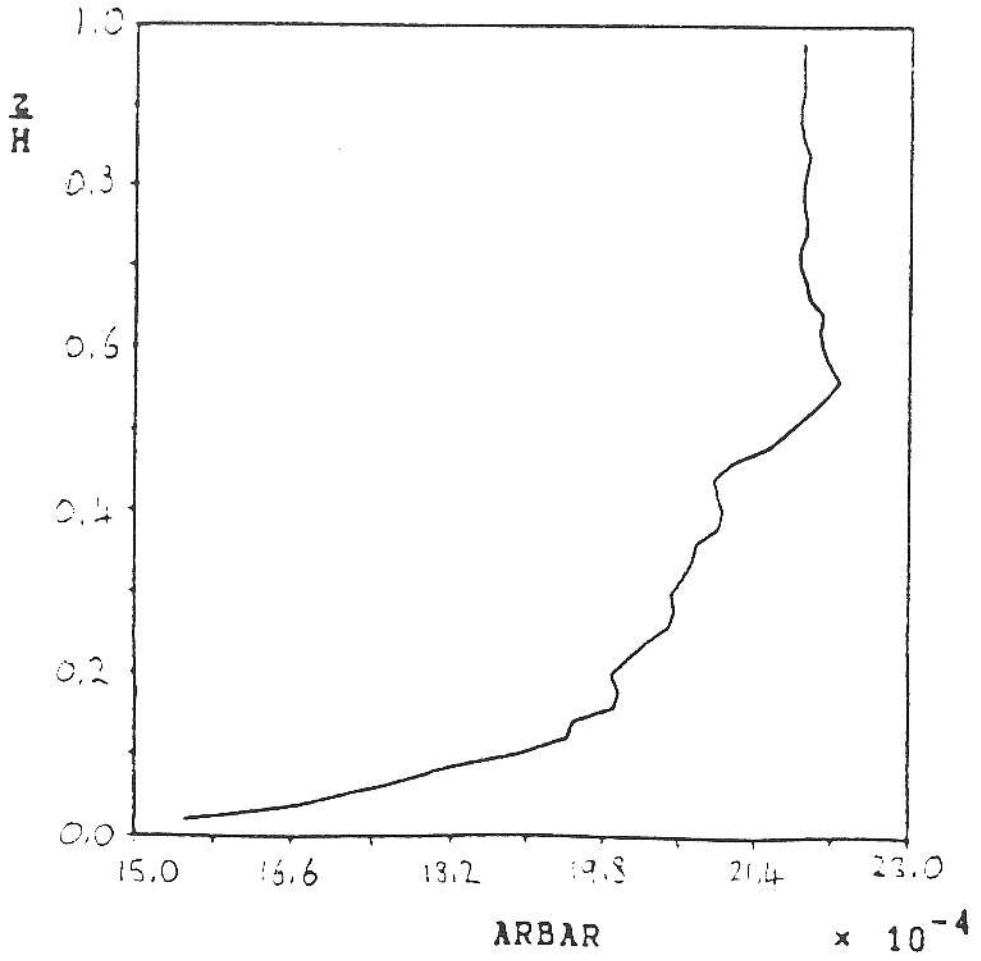

FIGURE 9. Mean linear-area occupied by segments above Specific Humidity threshold.

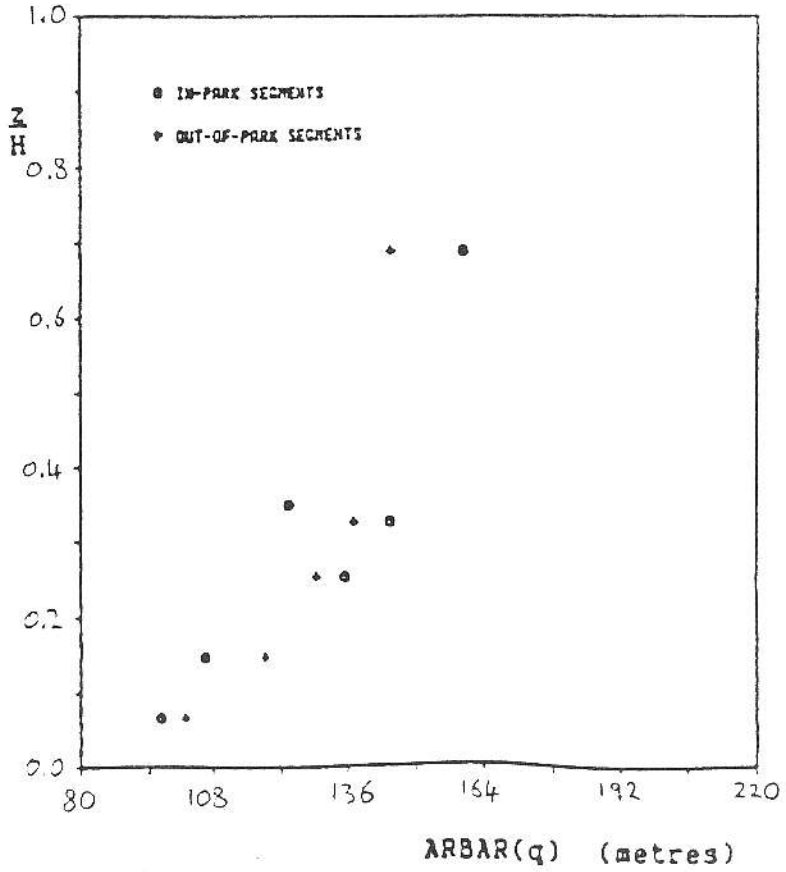

thermal fields into the model, and propagating them in different ways into the CBL, are made easily possibly.

It is expected, in the future, that the work in this report will be useful in the study of the Convective Boundary Layer over different surface heat fields. The ongoing work of F.I.A.M.S. over cleared and uncleared land on the Eyre Peninsula, and interests in the Lake Eyre and Coongie Lakes regions of North-Eastern South Australia, provide ample potential for such studies.

References

HACKER, J.M., 1982: First Results of Boundary Layer Research Flights with Three Powered Gliders During the Field Experiment PUKK. Beitr. Phys. Atmosph., 55, No. 4, Nov. 1982, 383-402.

HACKER, J.M., 1985: Flinders Research Aircraft: System description. Unpublished, July, 1985.

LENSCHOW, D.H., and STEPHENS, P.L., 1980: The Role of Thermals in the CBL. Bound. Layer Meteor., 19, 509-532.

MANTON, M.J., 1977: On the Structure of Convection. Bound. Layer Meteor., 12, 491-503.

MANTON, M.J., 1978: On Dry Penetrative Convection. Bound. Layer Meteor., 14, 301-322.

SCHWERDTFEGER, P., 1985: Chapter 6 of: Natural History of Eyre Peninsula, Roy. Soc. S.A., 89-100.

WARNER, J. and TELFORD, J.W., 1967: Convection Below Cloud Base. J. Atmos. Sci., 24, 374-382.

WILLIAMS, A.G., 1986: Dry Thermal Convection in a Well-Mixed Boundary Layer. BSc(Hon.) Thesis, Flinders Univ. of S.A.